JOURNAL OF MATERIALS SCIENCE 13 (1978) 2137–2146

Crystallization of grain boundary phases in hot-pressed silicon nitride materials

Part 1 *Preparation and characterization of materials*

J. E. WESTON*, P. L. PRATT, B. C. H. STEELE
Department of Metallurgy and Materials Science, Imperial College of Science and Technology, London, UK

Multicomponent oxide additions were used to replace magnesia as the densification aid for hot-pressing silicon nitride and silicon nitride–alumina materials. Crystallization of the silicate glass phases present after hot-pressing was encouraged by the use of an *in situ* heat treatment process. The phase constitutions of the materials produced by this method were determined using X-ray powder analysis. The kinetics of the densification of the silicon nitride materials were investigated, and these materials were examined using an X-ray diffractometer to study the textures produced by hot-pressing.

1. Introduction

Hot-pressed silicon nitride is produced commercially using magnesium oxide as a densification aid. The mechanical properties of this material at elevated temperatures are controlled by the presence of a magnesium silicate glass phase between the silicon nitride grains [1–9]. In particular, the reduction in the fracture strength at elevated temperatures, Fig. 1, seems to be caused by the subcritical growth of inherent flaws in the material due to stress-enhanced grain boundary sliding at the flaw tip [2]. Grain boundary sliding also causes the material to creep under an applied stress at elevated temperatures [7, 8]. The rate of grain boundary sliding at a given temperature is inversely related to the viscosity of the grain boundary glass phase so that any impurities in the silicon nitride that concentrate in the glass phase and lower its viscosity have a deleterious effect on the properties of the material. It has been found that impurities of calcium oxide have a particularly great effect on the high temperature mechanical properties of hot-pressed silicon nitride [2, 4].

In 1973, Gazza [10] showed that silicon nitride could be hot-pressed to a high density using yttrium oxide instead of magnesium oxide as the densification aid. The material produced by this method has a higher strength at elevated temperatures, as the grain boundary phase in this case is a yttrium silicate glass which is more refractory than a magnesium silicate glass. Rae *et al.* [11] found that yttrium oxide additions of greater than 10 wt % to silicon nitride produce a series of reactions during hot-pressing which lead to the formation of a crystalline yttrium silicon oxyntride ($Si_3N_4 \cdot Y_2O_3$) as the final grain boundary phase. The presence of a refractory crystalline phase at the grain boundaries gives the material a greatly improved high temperature strength and creep resistance. But the thermal expansion coefficient of the yttrium silicon oxynitride is approximately twice that of β-silicon nitride [11] so that its production at silicon nitride grain boundaries may lead to a highly stressed material with a poor resistance to thermal shock [12]. A further disadvantage of this technique is the relatively high viscosity of the yttrium silicate liquid phase produced during hot-pressing which necessitates the use of a high hot-pressing temperature (1750 to 1850° C) in order to obtain a fully dense, strong ceramic material.

*Present address: Department of Metallurgy and Materials Science, University of Cambridge, Pembroke Street, Cambridge, UK.

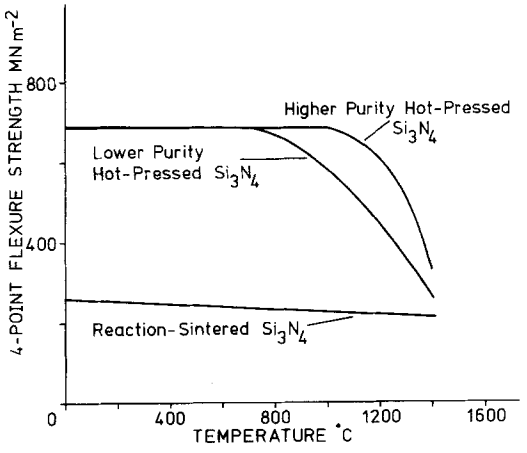

Figure 1 Effect of temperature on the fracture strength of silicon nitride ceramics (after [2] and [9]).

1.1. Design of a grain boundary phase for silicon nitride

The ideal hot-pressing additive for silicon nitride would form a liquid at the hot-pressing temperature to allow the silicon nitride to densify via liquid-phase sintering and would then form a crystalline phase, either when densification was complete or during cooling from the hot-pressing temperature. This crystalline phase should have the following characteristics:

(a) It must be crystallized from a glassy phase that will wet the silicon nitride particles and so allow densification via liquid-phase sintering during hot-pressing.

(b) It must crystallize from the glassy phase without a large change in the specific volume, as such a volume change would produce stresses in the final material which may be detrimental to its strength.

(c) It must have a thermal expansion coefficient close to that of β-silicon nitride (approximately $3.2 \times 10^{-6}\,°C^{-1}$).

(d) Ideally it should also have good mechanical properties so that the strength of the grain boundary is enhanced by crystallization.

These requirements are best met by a glass-ceramic containing α-cordierite ($2MgO \cdot 2Al_2O_3 \cdot 5SiO_2$) as its major phase. This phase can be crystallized from glasses in the $MgO-Al_2O_3-SiO_2$ system close to the compositoin of cordierite but with up to 5 wt% calcium oxide added [13–17].

Such ternary or quarternary glasses are less refractory than the usual magnesia–silica glasses produced during the hot-pressing of silicon nitride with magnesia additions. Thus the use of such glasses as the densification aid for hot-pressing silicon nitride may enable a strong, dense material to be obtained at a lower hot-pressing temperature than that commonly used for the hot-pressing of silicon nitride–magnesia mixtures.

2. Experimental

2.1. Starting materials

Two types of silicon nitride powder were used for this investigation, both powders being supplied by Advanced Materials Engineering Ltd. Typical impurity analyses of these powders (supplied by the manufacturer) are given in Table I.

X-ray powder analysis showed that the "controlled phase" powder contained 68% α-silicon nitride and 32% β-silicon nitride and the "high purity" powder contained 89% α-silicon nitride and 11% β-silicon nitride. No other crystalline phase was detected in the X-ray diffraction pattern of either grade of powder.

Both grades of silicon nitride powder were analysed to determine the amount of amorphous silica on the silicon nitride particles using a method developed by Colquhoun *et al.* [18]. It was found that the "controlled phase" powder contained 2.5 ± 0.2 wt% silica while the "high purity" powder had a silica content of 3.9 ± 0.2 wt%.

2.2. Hot-pressing additives

In an attempt to produce a material with a cordierite glass-ceramic as the grain boundary phase the hot-pressing additives were designed to produce a liquid phase in the material during hot-pressing which had a composition close to that of cordierite. As both the grades of silicon nitride used contained amorphous silica it was necessary to take these silica contents into account when designing the compositions of the densification additives.

Additive I, used with the "controlled phase" powder had the composition: 28.6 wt% SiO_2,

TABLE I Typical impurity analyses of silicon nitride powders

Powder grade	Typical impurity content (p.p.m.)					
	Al	Ca	Fe	Mg	K	Na
"Controlled phase"	6000	3000	9000	Impurity level unknown		
"High purity"	1200	400	650	80	34	11

34.3 wt% Al_2O_3, 5.8 wt% CaO, 17.1 wt% MgO and 14.1 wt% TiO_2. The titanium dioxide was included for two purposes:

(a) It is a well-known nucleating agent used in the production of cordierite glass-ceramics [15, 17].

(b) It is an intermediate oxide [19] which controls the viscosity of the liquid phase present at the hot-pressing temperature.

Additive I also contained calcium oxide to ensure a relatively high calcium oxide content in the material prepared from the "controlled phase" silicon nitride (calcium content up to 3000 p.p.m.). This allowed a comparison to be made between this material and the low calcium oxide content material prepared from the "high purity" powder. The crystallization of glasses in the Al_2O_3–CaO–MgO–SiO_2 system, for calcium oxide contents up to 5 wt%, is known to be similar to that for the Al_2O_3–MgO–SiO_2 system for compositions close to that of cordierite [14–16].

Additive II, used with the "high purity" powder had the composition 16.1 wt% SiO_2, 44.0 wt% Al_2O_3, 21.8 wt% MgO and 18.1 wt% TiO_2.

Both the additives were prepared from AnalaR grade chemicals except for the silica which was crushed Brazilian quartz and the titanium dioxide which was supplied by British Titan Products (>99% TiO_2). The additives were incorporated into the silicon nitride powders in the form of prefused mixtures to ensure that the additives were homogeneous. The oxide mixtures were fused at 1450° C for 3 h in a platinum crucible, water quenched and then crushed. This process was repeated twice and the fused mixtures were finally sieved and the fractions passing through 300 BSS mesh retained.

To investigate the phases produced by crystallization of the liquid phases formed by these additives a glass was prepared with the composition 44.5 wt% SiO_2, 26.7 wt% Al_2O_3, 4.5 wt% CaO, 13.3 wt% MgO and 11.0 wt% TiO_2. This is the composition of Additive I together with the surface silica content of the "controlled phase" silicon nitride powder when the proportions of silicon nitride and additive are the same as those used in this study (see Section 2.3). The glass was prepared using the same method as for the prefused additives except that, at the end of the third melting period, the molten glass was cast on a clean brass plate. The cast glass disc was transferred to a furnace set at 1100° C while it was still soft and left in this furnace for 3 h to allow the crystallization to go to completion. The resulting glass-ceramic was cooled slowly to room temperature. This product was designated "crystallized additive glass".

2.3. Powder preparation

The compositions of the powders used in this study are summarized in Table II.

Composition B consisted of "controlled phase" silicon nitride mixed with Additive I in the proportion of 8.74 g of Additive I to 100 g of silicon nitride. This addition, together with the surface silica content of the silicon nitride powder, gave the following nominal composition for the liquid phase present during the hot-pressing: 44.5 wt% SiO_2, 26.7 wt% Al_2O_3, 4.5 wt% CaO, 13.3 wt% MgO, 11.0 wt% TiO_2. The total silica content of this mixture was 5 wt%.

Composition J consisted of "high purity" silicon nitride mixed with Additive II in the proportion of 6.83 g of Additive II to 100 g of silicon nitride. Including the surface silica present in the silicon nitride powder, this addition gave a liquid phase during hot-pressing with the nominal com-

TABLE II Summary of powder compositions

Powder code letter	Si_3N_4 including surface SiO_2 (wt%)	SiO_2 (wt%)	Al_2O_3 (wt%)	CaO (wt%)	MgO (wt%)	TiO_2 (wt%)
B	91.96	2.29	2.76	0.47	1.38	1.14
J	93.61	1.02	2.81	0	1.40	1.16
C	38.65	0.96	59.13	0.20	0.58	0.48
E	47.91	1.20	49.34	0.24	0.72	0.59
F	57.01	1.43	39.72	0.29	0.85	0.70
G	65.96	1.65	30.25	0.33	0.99	0.82
H	74.77	1.87	20.94	0.38	1.12	0.92
I	83.43	2.13	11.74	0.42	1.25	1.03
K	93.16	1.02	2.80	0.47	1.39	1.16

position 46.6 wt% SiO_2, 28.0 wt% Al_2O_3, 13.9 wt% MgO and 11.5 wt% TiO_2. The total silica content of this mixture was also 5 wt%.

A series of powders (code letters C, E, F, G, H and I) was made up based on composition B with the addition of 60, 50, 40, 30, 20 and 10 wt% alumina, in addition to the alumina content of Additive I.

To investigate the effect of calcium oxide on the phases produced during hot-pressing, a sample of powder (code letter K) was made up from "high purity" silicon nitride with an additive which gave the following nominal liquid phase composition: 44.5 wt% SiO_2, 26.7 wt% Al_2O_3, 4.5 wt% CaO, 13.3 wt% MgO, 11.0 wt% TiO_2. In this case also, the total silica content of the mixture was 5 wt%.

The silicon nitride powder was mixed with the required amount of additive by grinding in distilled water in a mill with an alumina container and alumina grinding elements. The resultant slurry was dried and the dry powder was passed through a 300 mesh sieve to break up any agglomerates formed after milling.

2.4. Hot-pressing of powders

Two types of hot-pressing equipment were used in this study [20]. The vacuum press used a boron nitride lined graphite die with a 12.7 mm bore diameter which was positioned in an evacuated chamber and heated by r.f. induction. The graphite lower support of the die contained an axial hole which acted as a sighting hole for an optical pyrometer and so allowed the die temperature to be measured accurately. By manually controlling the power supplied to the r.f. induction coil, the die temperature could be controlled within approximately ±10° C. A known pressure could be applied to the upper plunger in the die via a spring-loaded beam. The powder charge for this vacuum hot-press was a stack of cold-pressed pellets which had been pressed at 351 MN m^{-2} in a steel die at room temperature without the use of any pressing binder. The densification of the compact during hot-pressing was measured by following the downward movement of the upper plunger in the die using a dial gauge dilatometer.

The large-scale press was based on a conventional 100 kN laboratory hydraulic press. The boron nitride lined graphite die had an internal diameter of 38 mm and was heated by r.f. induction. A "floating die" arangement was used and the die and plungers were surrounded by alumina powder which acted as thermal insulation and protected the graphite components from excessive oxidation. The die temperature was measured using a Pt/Pt–13% Rh thermocouple in thermal contact with the outside wall of the die. As for the vacuum hot-press, the die temperature could be controlled within approximately ±10° C. The powder charge was placed in the graphite die and cold-pressed *in situ* at 22.5 MN m^{-2} before the die was positioned in the hot-press. The densification of the powder compact during hot-pressing was followed by a dial gauge dilatometer in contact with the lower platen of the press frame.

A standard hot-pressing schedule was used in both hot-presses, i.e.:

(1) Gradual heating, room temperature to 1600° C, applied pressure 12.5 MN m^{-2}.

(2) 60 min at 1600° C, applied pressure 22.5 MN m^{-2}.

(3) Gradual cooling to <700° C, applied pressure 12.5 MN m^{-2}.

(4) Gradual heating to 1100° C, applied pressure 12.5 MN m^{-2}.

(5) 60 min at 1100° C, applied pressure 12.5 MN m^{-2}.

(6) Gradual cooling to room temperature, no applied pressure.

The compact was cooled to below 700° C after hot-pressing to allow any nucleation of crystalline phases in the glassy grain boundary layer produced during hot-pressing to occur under favourable conditions. The 60 min heat-treatment at 1100° C was used to encourage the growth of any such crystalline phases within the compact.

2.5. Density measurements

The density of each of the hot-pressed compacts was measured after the outer surfaces of the pellet had been lightly ground to remove any boron nitride contamination.

The compact density was found by the displacement method, using distilled water as the displacement medium. Comparison between values obtained by this method and those found by measuring and weighing machined samples of selected pellets showed that the former results were only about 1 to 2% greater than the latter. In view of the good agreement between these methods the displacement method was used in this study due to its convenience in practice.

2.6. X-ray analysis

X-ray powder analysis was carried out on the additive materials, the crystallized additive glass and the hot-pressed compacts. A Guinier asymmetric focusing powder camera was used with either CoKα or CuKα radiation. As the Guinier camera included a bent crystal monochromator this method gave diffraction patterns with very little background scattering which facilitated the detection of faint diffraction lines due to trace constituents in a sample. The powder diffraction patterns were measured using a split-beam neutral wedge photometer.

Polycrystalline samples of compositions B and J (Section 2.3) which had been hot-pressed in the large-scale press were used to prepare parallel-sided slices of material with their large faces parallel or perpendicular to the hot-pressing direction. These specimens were analysed using a standard X-ray diffractometer employing CuKα radiation with a 1° collimating slit, a $\frac{1}{2}$° receiving slit and a scanning speed of $\frac{1}{2}$° (2θ) per minute.

3. Results

3.1. Densification of compacts

Typical final densities of the various compositions studied are listed in Table III.

TABLE III Final densities of hot-pressed compacts

Composition	Hot-press used	Final density ($Mg\,m^{-3}$)
B	Vacuum	3.13
J	Vacuum	3.17
K	Vacuum	3.16
B	Large-scale	3.11
J	Large-scale	3.15
C	Vacuum	3.06
E	Vacuum	2.99
F	Vacuum	3.03
G	Vacuum	3.06
H	Vacuum	3.06
I	Vacuum	3.08

Using the readings of compact shrinkage obtained during hot-pressing, plots were drawn of compact density against time at the hot-pressing temperature for compositions B and J, Fig. 2. Graphs of the logarithm of the fractional densification of the compact against the logarithm of the hot-pressing time were constructed, Fig. 3. In each case a least-squares fit was calculated for the initial portion of the curve, disregarding the first reading just after the application of the full pressure at the start of hot-pressing. The slopes of these straight line portions are shown in Table IV.

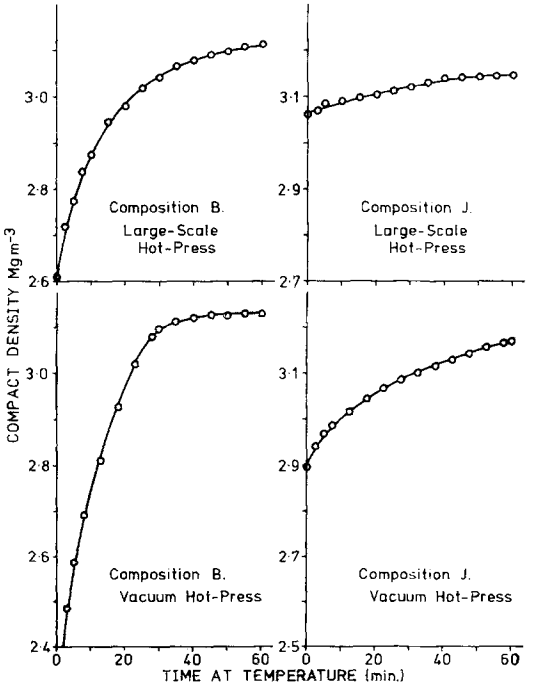

Figure 2 Compact density versus time at hot-pressing temperature, compositions B and J.

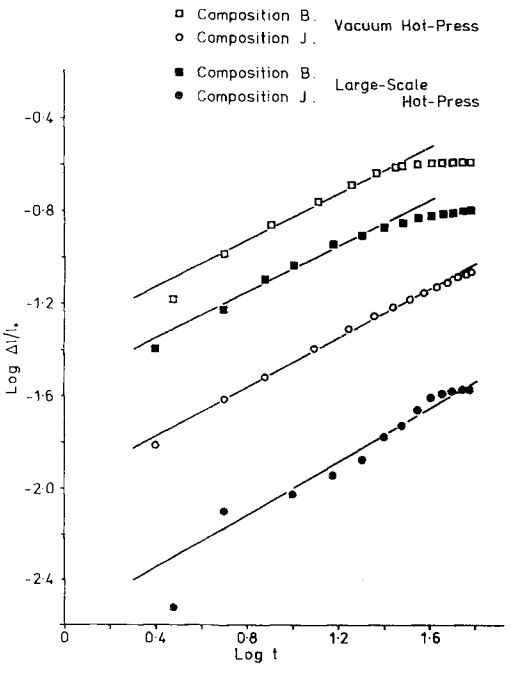

Figure 3 Logarithm (fractional densification) versus logarithm (hot-pressing time), compositions B and J.

TABLE IV Slopes of plots of logarithm (fractional densification) versus logarithm (hot-pressing time)

Composition	Hot-press used	Slope of straight line portion	Correlation coefficient
B	Vacuum	0.51	0.997
B	Large-scale	0.50	0.991
J	Vacuum	0.53	0.997
J	Large-scale	0.58	0.978

3.2. X-ray analysis

The crystalline phases identified by X-ray powder analysis of the additive materials, the crystallized additive glass and the hot-pressed compacts are summarized in Table V.

The X-ray diffractometer traces, obtained for sections parallel and perpendicular to the hot-pressing direction for samples of compositions B and J (Section 2.6), were found to consist of the diffraction patterns due to the phase mixture identified by X-ray powder analysis in each case. For each trace the diffraction peak heights of selected reflections in the β-silicon nitride and silicon oxynitride diffraction patterns were measured in arbitrary units and compared with the relative peak heights for a random powder sample, obtained from the Powder Diffraction File, Table VI.

4. Discussion

4.1. Densification of compacts

The final densities of the hot-pressed compacts, see Table III, appear to depend upon the compact composition and the type of hot-press used.

For compositions B and J the final density obtained is greater when the compact is prepared in the vacuum hot-press than in the large-scale press, in which there is no control of the atmosphere surrounding the compact. This is possibly due to gas trapped in pores in the compact in the large-scale press which would hinder the elimination of the pores during densification. In the vacuum hot-press the powder compact is evacuated before the application of pressure. Therefore, except for the

TABLE V Summary of X-ray powder analysis data

Composition	Hot-press used (where applicable)	Crystalline phases detected by X-ray powder analysis
Additive I	–	Spinel, *major*; titanium dioxide (rutile), *minor*.
Additive II	–	Spinel, *major*; β-aluminium titanate, *minor*.
Crystallized additive glass	–	α-cordierite, *major*; μ-cordierite, *trace*.
B	Vacuum	β-silicon nitride, *major*; forsterite, *minor*; silicon, *minor*.
B	Large-scale	β-silicon nitride, *major*; forsterite, *minor*; silicon oxynitride, *minor*; silicon, *trace*.
J	Vacuum	β-silicon nitride, *major*; silicon oxynitride, *minor*; enstatite, *minor*.
J	Large-scale	β-silicon nitride, *major*; silicon oxynitride, *medium*, enstatite, *minor*.
K	Vacuum	β-silicon nitride, *major*; silicon oxynitride, *minor*, enstatite, *minor*.
C E	Vacuum	β′-phase, *major*; X-phase, *medium*; α-alumina, *minor*; forsterite, *minor/trace*.
F G	Vacuum	β′-phase, *major*; X-phase, *minor* forsterite, *minor*; α-alumina, *minor*.
H I	Vacuum	β′-phase, *major*; X-phase, *minor*; forsterite, *minor*.

β-silicon nitride = β-Si_3N_4; β′-phase = $Si_{6-x}Al_xO_xN_{8-x}$; silicon oxyntride = Si_2ON_2; forsterite = Mg_2SiO_4; enstatite = $MgSiO_3$; α-alumina = α-Al_2O_3; cordierite = $2MgO \cdot 2Al_2O_3 \cdot 5SiO_2$; spinel = $MgAl_2O_4$; rutile = TiO_2; β-aluminium titanate = β-Al_2TiO_5.

TABLE VI(a) Comparison of X-ray diffraction peak heights for β-silicon nitride

h k l	Composition B		Composition J		
	I^* ∥ H-P axis	I^* ⊥ H-P axis	I^* ∥ H-P axis	I^* ⊥ H-P axis	$\frac{I^\dagger}{I_0}$
100	29	23	31	42	18
110	50	39	50	59	20
200	154	120	154	184	85
101	249	72	247	157	100
210/120	193	143	194	231	100
201	81	34	83	66	35
310	29	24	31	37	20
301	103	57	104	98	70
221	34	32	37	40	20

*I = arbitrary units minus background.
†I/I_0 = standard values from Powder Diffraction File.

TABLE VI(b) Comparison of X-ray diffraction peak heights for silicon oxynitride

h k l	Composition B		Composition J		
	I^* ∥ H-P axis	I^* ⊥ H-P axis	I^* ∥ H-P axis	I^* ⊥ H-P axis	$\frac{I^\dagger}{I_0}$
110	3.5	2.5	11	14	80
200	4.0	6.0	18	49	100
111	3.5	4.0	43	23	100
310	3.0	4.5	15	30	50
002	5.0	2.0	31	10	80
021	7.0	3.0	24	13	80

*I = arbitrary units minus background.
†I/I_0 = standard values from Powder Diffraction File.

possibility of the presence of some silicon monoxide gas due to the partial reduction or dissociation of the surface silica on the silicon nitride grains, the only gas present in the pores during hot-pressing would be due to the decomposition of silicon nitride:

$$Si_3N_4 \rightarrow 3Si + 2N_2 \uparrow \quad (1)$$

The densities of the materials based on composition B with the addition of 10 to 60 wt% alumina, see Table III, are lower than those of compositions B and J but are similar to the densities of simple mixtures of "controlled phase" silicon nitride with 20 to 60 wt% alumina which have been hot-pressed under similar conditions, Table VII. As all the hot-pressed compositions result in products containing more than one phase (Section 4.2) it is not possible to express the densities of these products as a proportion of a theoretical density calculated from X-ray data. However, the densities of compositions B and J are as great as or greater than the densities of hot-pressed silicon nitride–magnesia materials at a similar stage in their development [21].

TABLE VII Final densities of "controlled phase" silicon nitride–alumina compacts hot-pressed at 1600° C, 22.5 MN m^{-2} for 60 min, no heat-treatment

Composition	Hot-press used	Final density (Mg m^{-3})
Si_3N_4 –20 wt % Al_2O_3	Vacuum	2.90
Si_3N_4 –40 wt % Al_2O_3	Vacuum	3.03
Si_3N_4 –60 wt % Al_2O_3	Vacuum	2.99

From the plots of compact density against hot-pressing time for compositions B and J, Fig. 2, it can be seen that there is more densification of the compact before the hot-pressing temperature is reached and the full pressure applied when the large-scale press is used. This is due to the longer heating time required for the large-scale press. Also, whichever hot-press is used, there is more densification during the heating period for composition J compacts but the densification rate of composition B compacts is greater once the hot-pressing temperature is reached and the full load applied.

The densification of these compacts can be interpreted in terms of the theory of liquid phase sintering proposed by Kingery [22]. If it is assumed that only the first stage of densification, i.e. the particle rearrangement process, occurs during the heating period, then the above data suggest that composition J produces a compact with a higher total liquid content than that of composition B compacts below 1600° C. But the initial particle rearrangement in these materials may be influenced to a greater degree by the softening or dissolution of the probably amorphous silica layers on the silicon nitride particles, rather than by their total liquid phase contents. Softening or removal of these surface layers would facilitate the movement of the solid grains over one another. Therefor the greater initial densification of composition J may reflect the higher surface silica content of the silicon nitride powder ("high purity" powder) used to prepare this material.

The slopes of the initial portions of the log–log plots of fractional compact densification against hot-pressing time for compositions B and J, Table IV, were found to be approximately +0.5 in each case. This corresponds to the relationship:

$$\frac{\Delta l}{l_0} \propto t^{1/2} \quad (2)$$

where:

l_0 = length of compact at the start of hot-pressing

Δl = change in length of the compact
t = time at the hot-pressing temperature and pressure.

This agrees with the theoretical rate of densification for a solution–precipitation process. The rate-determining step is the reaction at the phase boundary leading to dissolution at the solid particle contact points, for a compact with spherical particles [22]*.

Investigations of the hot-pressing and sintering behaviour of silicon nitride–magnesia mixtures [23–25] have led to the relationship:

$$\frac{\Delta l}{l_0} \propto t^{1/n} \qquad (3)$$

where n varies from 3 to 5. These results suggest that the overall kinetics are controlled by either diffusion through the liquid phase or the reaction at the phase boundary, depending on the amount and viscosity of liquid phase present during densification.

For compositions B and J the liquid phases present at the hot-pressing temperature are multicomponent glasses which would have lower viscosities than the relatively simple liquid phase present in silicon nitride–magnesia mixtures. Thus diffusion through the liquid phase should be faster for compositions B and J than for silicon nitride–magnesia compacts. For these more complex materials therefore the rate-determining step for densification is always the dissolution of silicon nitride into the liquid phase at the interparticle contacts.

The deviation from linearity at longer hot-pressing times shown in the plots of log $(\Delta l/l_0)$ against log t, Fig. 3, was also found by Terwilliger and Lange [23] for silicon nitride–magnesia compacts. This reduction in the rate of densification is due to the gradual coalescence of the solid particles in the compact. This causes the cessation of sintering by a liquid phase mechanism so that the densification rate gradually reduces to that for a solid state process.

4.2. X-ray analysis

The results of the powder diffraction analysis of the additives, see Table V, confirm that there is mixing of the oxide constituents during the periods of heating at 1450° C. The silica in each additive is either incorporated in a solid solution with one of the crystalline phases or is present in a glass phase.

The analysis of the crystallized additive glass (Section 2.2) shows this product to consist of the α-phase modification of cordierite ($2MgO \cdot 2Al_2O_3 \cdot 5SiO_2$) with a trace constituent of μ-cordierite. This suggests that the initial crystallization product is μ-cordierite in agreement with the findings of Zdaniewski [17]. As μ-cordierite is the low-temperature polymorph it would transform to the high-temperature form, i.e. hexagonal α-cordierite, during the heat-treatment at 1100° C.

Although the crystallized additive glass shows that glasses similar in composition to the computed nominal compositions of the grain boundary phases in powders B, J and K will give cordierite on crystallization at 1100° C, in no case was cordierite detected in the products of hot-pressing these powders, Table V. For compositions B and J it was found that the hot-pressing conditions affected the constitution of the final products.

When prepared in the vacuum hot-press, composition B contains forsterite (Mg_2SiO_4) as a minor phase but composition J contains silicon oxynitride and enstatite ($MgSiO_3$). Forsterite and enstatite are possible crystallization products for glass compositions containing less alumina than those which give cordierite on crystallization. Thus it appears that the alumina present in the additives used for compositions B and J must react with the silicon nitride during hot-pressing to form the β'-phase ($Si_{6-x}Al_xO_xN_{8-x}$) [26].

If all the alumina was incorporated into the β'-phase the values of "x" would be 0.164 for composition B and 0.167 for composition J.

There are at least three possible explanations for the different minority phases produced in compositions B and J on hot-pressing:

(a) The calcium oxide content of composition B is much greater than that of composition J, (Sections 2.1 and 2.2). However, composition K, which consists of the "high purity" silicon nitride (as for composition J) and an additive with the same calcium oxide content as that used for composition B, gives a hot-pressed product with an

*The use of Kingery's analysis [22] for the kinetics of densification of silicon nitride is questionable as in this case there is a phase change occurring during the solution–reprecipitation process (i.e. α- to β-silicon nitride). Thus the driving force for densification may be the difference in free-energy between α- and β-silicon nitride and not the enhanced solubility of the solid phase at the interparticle contact points. However, this analysis is used here to allow comparison with literature data for conventional hot-pressed silicon nitrides which have been interpreted using Kingery's model for densification.

X-ray diffraction pattern virtually identical to that of composition J. The presence of calcium oxide at the level used in this case appears to have little or no effect on the phase constitution of the hot-pressed products.

(b) The surface silica content of "high purity" silicon nitride powder is approximately 1.6 times that of the "controlled phase" powder (Section 2.1). Thus although both compositions (B and J) have a final silica content of 5 wt %, half the silica content of composition B before hot-pressing is at a reduced activity, as it is dissolved in the mixture of fused oxides making up the additive, while for composition J before hot-pressing only about one fifth of the total silica content is at a reduced activity. The relatively large proportion of high activity silica in composition J may encourage the formation of silicon oxynitride by a reaction such as:

$$SiO_2 + Si_3N_4 \rightarrow 2Si_2ON_2 \qquad (4)$$

Although this may explain the presence of silicon oxynitride in composition J it does not directly explain why enstatite is formed in this composition and forsterite in composition B.

(c) There may have been an error in the analysis of the silicon nitride starting powders for surface silica, due to either experimental error or a difference in the solubilities of the surface silica layers in the sodium hydroxide solution used in the analysis. Thus there may be a difference in the true total silica contents of the powders leading to the formation of different minority phases on hot-pressing and subsequent heat treatment.

Using the large-scale hot-press, composition B contains forsterite and silicon oxynitride as minor phases while composition J contains enstatite and silicon oxynitride, with a larger proportion of silicon oxynitride present than for the material hot-pressed in vacuum. The environment in the large-scale press must contain a higher oxygen partial pressure than in the vacuum hot-press. A relatively high oxygen partial pressure would encourage the formation of silicon oxynitride in thermodynamic equilibrium with β-silicon nitride [27].

For the materials based on composition B with the addition of 10 to 60 wt % alumina, which were all hot-pressed in the vacuum press, the X-ray analysis results reveal a systematic variation in the crystalline phases present as the alumina content increases, see Table V. In each case the silicate phase given by the crystallization of the grain boundary glass is forsterite and not cordierite. This suggests that the silicate phase crystallizes from a glass that is deficient in alumina.

During the hot-pressing of these materials there is a reaction between the α-alumina and silicon nitride to form β'-phase, a solid solution of AlN–Al_2O_3 in β-Si_3N_4 [26]. There is also a reaction between the α-alumina, silicon nitride and silica to form X-phase, which has been described as a nitrogen containing mullite with a composition close to $SiAlO_2N$ [28]. It seems likely that these reactions take place by the gradual dissolution of the reactants into the liquid phase present at the hot-pressing temperature and subsequent precipitation of the products in a manner similar to that proposed for the silicon nitride–magnesia system [29]. Thus, at the end of the hot-pressing period, this liquid phase would contain a limited amount of alumina and, if the X-phase is preferentially precipitated on cooling from the hot-pressing temperature, the remaining grain boundary phase would be alumina deficient. Subsequent crystallization of the grain boundary phase would then be likely to give a magnesium silicate such as forsterite.

Tables VIa and b show the peak heights of selected β-silicon nitride and silicon oxynitride diffraction peaks for samples of compositions B and J hot-pressed in the large-scale press. For both compositions these peak heights differ significantly from the intensities given by a random powder and hence from the intensities that would be given if hot-pressing produced an isotropic material with randomly oriented grains. The diffraction patterns of β-silicon nitride and silicon oxynitride obtained from sections normal to the hot-pressing direction both show a decrease in peak height for reflections from planes which intersect the c-axis of the β-silicon nitride or silicon oxynitride unit cell respectively. Thus there is a preferred orientation or texture produced on hot-pressing compositions B and J, i.e. the β-silicon nitride and silicon oxynitride grains tend to align so that the c-axis in each case is perpendicular to the hot-pressing direction. A similar effect has been noted for β-silicon nitride in hot-pressed silicon nitride–magnesia materials [30, 31].

5. Conclusions

(1) Silicon nitride and silicon nitride–alumina materials can be hot-pressed to high density at 1600° C using a densification aid consisting of a

multi-component oxide mixture such as "Additive I" or "Additive II". This temperature is lower than the usual hot-pressing temperature of silicon nitride–magnesia mixtures.

(2) For the silicon nitride materials the densification mechanism during hot-pressing appears to be a solution–precipitation process via the liquid phase, with the rate-determining step being the dissolution of material at the particle contact points.

(3) X-ray analysis of the materials prepared in this study suggests that it is possible to induce at least partial crystallization of the glass phases produced during hot-pressing although the crystallization product is a magnesium silicate and not cordierite, even in materials containing large excesses of alumina.

(4) Hot-pressing produces an anisotropic material, i.e. there is a tendency for both β-silicon nitride and silicon oxynitride grains to be aligned so that their c-axes are perpendicular to the hot-pressing direction.

Acknowledgements

We are grateful to the glass-ceramics group in the Metallurgy and Materials Science Department of Imperial College, especially Dr P. S. Rogers, for their kind assistance in the preparation of the hot-pressing additives. J. Weston was supported by a Science Research Council Research Studentship from 1973 to 1976.

References

1. W. ASHCROFT, "Special Ceramics", Vol. 6, edited by P. Popper (British Ceramic Research Association, Stoke-on-Trent, 1975) p. 245.
2. F.F. LANGE, *J. Amer. Ceram. Soc.* **57** (1974) 84.
3. S.D. HARTLINE, R.C. BRANDT, D.W. RICHARDSON and M.L. TORTI, *ibid.* **57** (1974) 190.
4. J.L. ISKOE, F.F. LANGE and E.S. DIAZ, *J. Mater. Sci.* **11** (1976) 908.
5. J.L. HENSHALL, D.J. ROWCLIFFE and J.W. EDINGTON, "Special Ceramics", Vol. 6, edited by P. Popper (British Ceramic Research Association, Stoke-on-Trent, 1975) p. 185.
6. J.J. PETROVIC, L.A. JACOBSON, P.K. TALTY and A.K. VASUDEVAN, *J. Amer. Ceram. Soc.* **58** (1975) 113.
7. R. KOSSOWSKY, D.G. MILLER and E.S. DIAZ, *J. Mater. Sci.* **10** (1975) 983.
8. SALAH UD DIN and P.S. NICHOLSON, *ibid.* **10** (1975) 1375.
9. A.G. EVANS and J.V. SHARP, *ibid.* **6** (1971) 1292.
10. G.E. GAZZA, *J. Amer. Ceram. Soc.* **56** (1973) 662.
11. A.W.J.M. RAE, D.P. THOMPSON, N.J. PIPKIN and K.H. JACK, "Special Ceramics", Vol. 6, edited by P. Popper (British Ceramic Research Association, Stoke-on-Trent, 1975) p. 347.
12. G.E. GAZZA, *Ceram. Bull.* **54** (1975) 778.
13. A.G. GREGORY and T.J. VEASEY, *J. Mater. Sci.* **6** (1971) 1312.
14. R.C. DE VEKEY and A.J. MAJUMDAR, *Mineral. Mag.* **37** (1970) 771.
15. *Idem, Glass Technol.* **14** (1973) 125.
16. *Idem, Mater. Res. Bull.* 8 (1973) 1073.
17. W. ZDANIEWSKI, *J. Mater. Sci.* 8 (1973) 192.
18. I. COLQUHOUN, D.P. THOMPSON, W.I. WILSON, P. GRIEVESON and K.H. JACK, *Proc. Brit. Ceram. Soc.* **22** (1973) 181.
19. L.D. PYE, "Introduction to Glass Science", (Plenum Press, New York, London, 1972) p. 25.
20. J.E. WESTON, Ph.D. Thesis, London University (1977).
21. G.G. DEELEY, J.M. HERBERT and N.C. MOORE, *Powder Met.* 8 (1961) 145.
22. W.D. KINGERY, *J. Appl. Phys.* **30** (1959) 301.
23. G.R. TERWILLIGER and F.F. LANGE, *J. Amer. Ceram. Soc.* 57 (1974) 25.
24. M. MITOMO, *J. Mater. Sci.* **11** (1976) 1103.
25. I. AMATO, D. MARTORANA and B. SILENGO, *Mater. Sci. Eng.* **28** (1977) 215.
26. R.J. LUMBY, B. NORTH and A.J. TAYLOR, "Special Ceramics", Vol. 6, edited by P. Popper (British Ceramic Research Association, Stoke-on-Trent, 1975) p. 283.
27. K. BLEGEN, *ibid.* p. 223.
28. K.H. JACK, *J. Mater. Sci.* **11** (1976) 1135.
29. P. DREW, and M.H. LEWIS, *ibid.* 9 (1974) 261.
30. F.F. LANGE, *J. Amer. Ceram. Soc.* **56** (1973) 518.
31. K. NUTTALL and D.P. THOMPSON, *J. Mater. Sci.* 9 (1974) 850.

Received 28 November 1977 and accepted 15 February 1978.